Chemical Geology 385 (2014) 84–91

Contents lists available at ScienceDirect

Chemical Geology

journal homepage: www.elsevier.com/locate/chemgeo

Using stable Mg isotopes to distinguish dolomite formation mechanisms: A case study from the Peru Margin

Vasileios Mavromatis [a,*], Patrick Meister [b,**], Eric H. Oelkers [a,c]

[a] Geosciences Environment Toulouse (GET), CNRS, UMR 5563, Observatoire Midi-Pyrénées, 14 Av. E. Belin, 31400 Toulouse, France
[b] Max-Planck-Institut für Marine Mikrobiologie, Celsiusstr. 1, 28357 Bremen, Germany
[c] Department of Earth Sciences, University College London, Gower Street, WC1E 6BT, UK

ARTICLE INFO

Article history:
Received 6 January 2014
Received in revised form 21 July 2014
Accepted 21 July 2014
Available online 27 July 2014

Editor: Michael E. Böttcher

Keywords:
Early diagenesis
Dolomite formation
Mg isotopes
Pore fluid composition

ABSTRACT

The magnesium isotope composition of diagenetic dolomites and their adjacent pore fluids were studied in a 250 m thick sedimentary section drilled into the Peru Margin during Ocean Drilling Program (ODP) Leg 201 (Site 1230) and Leg 112 (Site 685). Previous studies revealed the presence of two types of dolomite: type I dolomite forms at ~6 m below seafloor (mbsf) due to an increase in alkalinity associated with anaerobic methane oxidation, and type II dolomite forms at focused sites below ~230 mbsf due to episodic inflow of deep-sourced fluids into an intense methanogenesis zone. The pore fluid δ^{26}Mg composition becomes progressively enriched in ^{26}Mg with depth from values similar to seawater (i.e. −0.8‰, relative to DSM3 Mg reference material) in the top few meters below seafloor (mbsf) to 0.8 ± 0.2‰ within the sediments located below 100 mbsf. Type I dolomites have a δ^{26}Mg of −3.5‰, and exhibit apparent dolomite-pore fluid fractionation factors of about −2.6‰ consistent with previous studies of dolomite precipitation from seawater. In contrast, type II dolomites have δ^{26}Mg values ranging from −2.5 to −3.0‰ and are up to −3.6‰ lighter than the modern pore fluid Mg isotope composition. The enrichment of pore fluids in ^{26}Mg and depletion in total Mg concentration below ~200 mbsf is likely the result of Mg isotope fractionation during dolomite formation, The ^{26}Mg enrichment of pore fluids in the upper ~200 mbsf of the sediment sequence can be attributed to desorption of Mg from clay mineral surfaces. The obtained results indicate that Mg isotopes recorded in the diagenetic carbonate record can distinguish near surface versus deep formed dolomite demonstrating their usefulness as a paleo-diagenetic proxy.

1. Introduction

Magnesium (Mg) isotope composition has been suggested to be a useful proxy for deducing mineral formation temperature, mineral growth rate, and identifying weathering regimes (Galy et al., 2002; Tipper et al., 2006; Pogge von Strandmann et al., 2008; Immenhauser et al., 2010; Pokrovsky et al., 2011; Li et al., 2012; Riechelmann et al., 2012; Mavromatis et al., 2012a, 2013; Shirokova et al., 2013). This element is abundant in seawater, silicate rocks, and many carbonate minerals; Mg-isotope fractionation among these phases is sufficiently large to distinguish natural processes (e.g. Young and Galy, 2004). In particular, the high concentration and the homogeneous chemical and isotopic distribution of Mg in modern seawater and its presence in biogenic and abiotic carbonates (Hippler et al., 2009; Wombacher et al., 2011; Yoshimura et al., 2011; Mavromatis et al., 2012a) make Mg-isotopes an excellent tool to trace oceanographic and biogeochemical conditions in the rock record. Notably, Mg-isotopes provide a promising tool to investigate the formation and diagenetic transformation of carbonate minerals.

With its high Mg concentration, dolomite [$MgCa(CO_3)_2$] offers one of the richest Mg archives, ideal for Mg isotopic studies. While much dolomite is formed during burial diagenesis and hydrothermal alteration, numerous examples of penecontemporaneous or early diagenetic dolomite have been reported (cf. examples reviewed in Meister et al., 2013). This latter dolomite is of particular interest as it may preserve paleo-ocean geochemical and isotopic signatures. In addition, Mg isotopes have the potential to reveal carbonate precipitation mechanism (Mavromatis et al., 2013) and, thus, may hold the key to understanding dolomite formation at near-Earth's surface conditions.

The goal of this study is to improve our understanding of Mg isotope fractionation between carbonate minerals and their coexisting fluids. At present, only a limited number of Mg-isotope datasets are available from carbonates that formed in either laboratory or natural systems (e.g. Galy et al., 2002; Young and Galy, 2004; Buhl et al., 2007; Hippler et al., 2009; Immenhauser et al., 2010; Pokrovsky et al., 2011; Mavromatis et al., 2012a, 2013; Azmy et al., 2013; Shirokova et al., 2013). While it is

* Correspondence to: V. Mavromatis, Institute of Applied Geosciences, Graz University of Technology, Rechbauerstrasse 12, 8010 Graz, Austria.
** Correspondence to: P. Meister, Department of Geodynamics and Sedimentology, University of Vienna, Althanstr. 14, 1090 Vienna, Austria.
E-mail address: mavromatis@tugraz.at (V. Mavromatis).

http://dx.doi.org/10.1016/j.chemgeo.2014.07.019
0009-2541/

generally accepted that carbonates preferentially incorporate light Mg, fractionation factors and their mechanistic controls are still poorly understood. Moreover, the degree to which reaction kinetics affects the fractionation among carbonate minerals and fluids remains unclear (cf. Immenhauser et al., 2010; Pearce et al., 2012; Mavromatis et al., 2013). This study builds upon these past efforts by characterizing the Mg-isotope compositions of dolomites and their adjacent pore fluids recovered from drill cores collected from the Peruvian Trench Ocean Drilling Program (ODP) Site 1230. This Site provides an ideal model case, as two distinct dolomite types are present, one at shallow and one at greater depths, where the Mg isotope composition of the dolomites can be studied together with those of their adjacent pore fluids.

2. Study site

This study focuses on the Mg isotope chemistry of two drill cores collected from the Peru Margin. The Peru Margin (Fig. 1) is one of the Earth's largest upwelling zones with deposition of large amounts of biogenic silica and organic matter. Site 1230 (9° 06.78′ S, 80° 35.01′ W) was drilled during ODP Leg 201 on the lower slope of the Peru Trench below 5086 m water depth, at the same location as Site 685 of Leg 112. Site 1230 is characterized by high sedimentation rates exceeding 100 m/my (Kastner et al., 1990) and organic carbon contents ranging from 2 to 4%. Its stratigraphic sequence consists of Miocene to Holocene diatom ooze, silt, and clay. At ~223 mbsf, the sequence is dissected by a décollement that formed due to tectonic activity within the Peruvian Trench accretionary complex (D'Hondt et al., 2003). A lithostratigraphic description of Sites 685 and 1230 is provided in the Electronic Supplementary Material (ESM) Fig. S1.

2.1. Pore fluid geochemistry

The pore fluid chemistry at Site 1230 is influenced by intense microbial activity with sulfate depletion above 10 mbsf, and strong methanogenic activity beneath (Kastner et al., 1990). Within the top 200 mbsf, this high activity resulted in the accumulation of up to 40 mM of NH_4 and ~300 mM of CH_4 (Spivack et al., 2006). At several depths, gas hydrates were observed (Inagaki et al., 2006). Alkalinity reaches ~150 mM at around 150 mbsf. Accordingly, dissolved inorganic carbon (DIC) production is high, but its exact concentration is difficult to measure, as some DIC may have degassed upon sampling. Since organic matter fermentation produces CO_2, the methanogenic zone is likely acidified (Meister et al., 2011). In addition, the methanogenic zone at this site also showed enrichment of dissolved organic carbon (DOC) up to 20 mM (Smith, 2005).

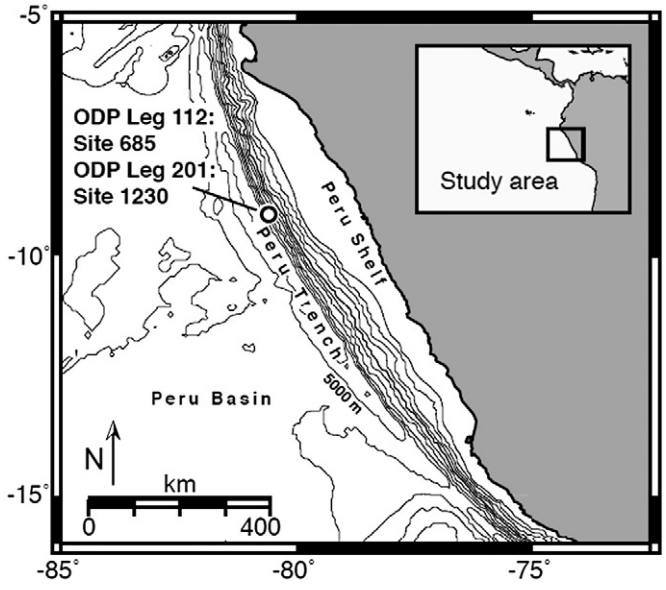

Fig. 1. Map of the Peru Margin showing the location of the drill Sites 685 and 1230 near the Trench axis, modified after Meister et al. (2011).

Chlorine concentration (Fig. 2) is close to constant with depth and similar to that of seawater with the exception of the depths at which gas hydrates occur. Pore fluid Mg concentrations (Fig. 2) show a similar distribution as the metabolites, while Ca concentrations show an opposite distribution. Pore fluid Ca concentration is depleted to ~4 mM at 13.6 mbsf (see Fig. 2) and remains as low down to 237 mbsf. Below this depth, aqueous Ca concentration increases to 17.8 mM at 450 mbsf (ODP 112, Site 685; Kastner et al., 1990). In contrast, the aqueous Mg concentration increases downward at Site 1230 from 55 mM (seawater composition) to ~70 mM at ~100 mbsf, but below this depth it decreases to 28 mM at 450 mbsf (ODP 112, Site 685; Kastner et al., 1990). The increase in Mg above seawater concentration, observed between 17 and 100 mbsf, has been interpreted to result from an exchange between ammonium and magnesium ions on clay mineral surfaces (Von Breymann et al., 1990; Donohue et al., 2006). Von Breymann et al. (1990) also argued that pore fluid Mg depletion below ~150 mbsf is the result of the formation of dolomite, which is abundant at this Site below ~230 mbsf (see Thornburg and Suess, 1992).

2.2. Authigenic dolomite formation

The carbonate content is generally low (0–5 wt.%; Suess et al., 1990) throughout the sediment sequence at Sites 1230 and 685 (Suess et al., 1990). Authigenic dolomites occur at ~6 mbsf and at several depths below ~230 mbsf; the dolomites from these two locations also differ in texture and formation process. They are here referred to as Type I and Type II dolomite, respectively. While the authigenic dolomite at ~6 mbsf is induced by the anaerobic oxidation of methane (AOM) based on its $\delta^{13}C$ composition (Meister et al., 2007), dolomite formation in the deeper strata is most likely induced by upward migrating fluids that buffered pH in the methanogenic zone (Meister et al., 2011). Upward fluid transport along the décollement has been observed (Matmon and Bekins, 2006) and further evidenced by the strongly radiogenic pore fluid $^{87}Sr/^{86}Sr$ ratios, suggesting interaction of the fluid with the continental basement at greater depth (Kastner et al., 1990; Meister et al., 2011). In fact, a wedge of continental basement is present beneath the sedimentary sequence at this site (Von Huene et al., 1996). This fluid was also enriched in ^{18}O due to clay mineral dehydration during smectite–illite transformation (cf. Hensen et al., 2004; Mavromatis et al., 2012b). Fluid migration is also consistent with the heavy oxygen isotope composition of pore fluids and precipitated dolomites (Meister et al., 2011).

3. Material and methods

3.1. Mineralogical and carbon/oxygen isotope analyses

The mineralogy of solid samples was characterized using a Philips XPERT pro X-ray diffractometer at University of Bremen. CuKα radiation was used and the samples were scanned from 3 to 85° (2θ) at a scan rate of 1.63°/min and a step size of 0.0167°. The proportions of different minerals were estimated from integrated peak areas. Total inorganic carbon (TIC) was measured using a CM 5012 CO_2 Coulometer (UIC) by acidification with 3 M phosphoric acid. Analytical precisions (2σ) were 0.2 wt.% for total carbon and 0.1 wt.% for TIC.

Carbon and oxygen isotopes in powdered bulk sediments were analyzed using a Finnigan MAT 251 mass spectrometer coupled to an automated acidification device (type "Kiel") at the Geological Institute, University of Bremen. The analytical precision of the mass spectrometer, based on repeated standard analyses, is ±0.05‰ for $\delta^{13}C$, and ±0.07‰ for $\delta^{18}O$. Powdered Solnhofener Plattenkalk, calibrated against the NBS standard, was used as a working standard and the $\delta^{13}C$ and $\delta^{18}O$ values

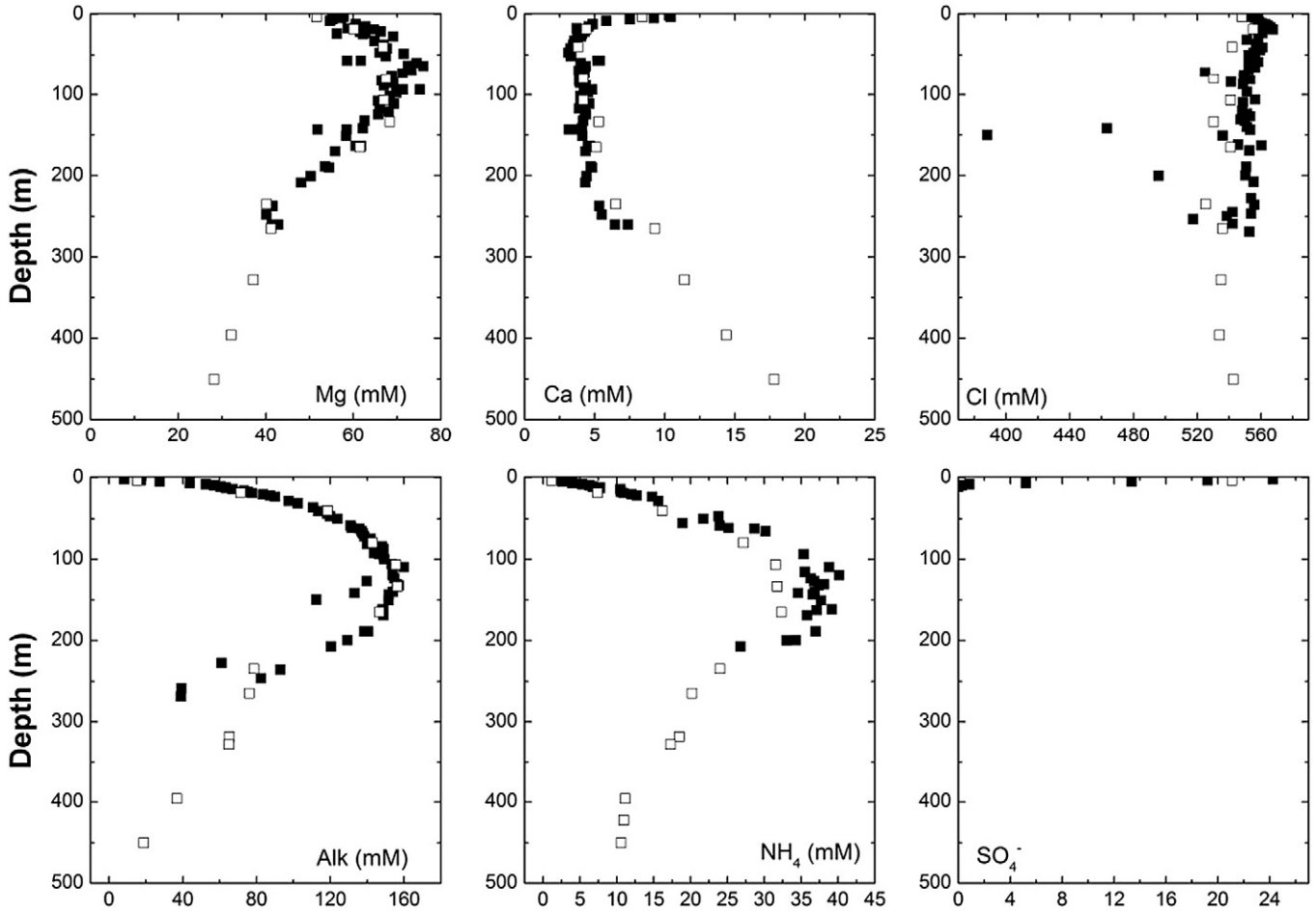

Fig. 2. Pore fluid depth–concentration profiles for Mg, Ca, Cl, alkalinity, NH_4^- and SO_4. Closed symbols, refer to data from Site 1230 (Leg 201) from D'Hondt et al. (2003) and Donohue et al. (2006). Open symbols refer to data from Site 685 (Leg 112) from Kastner et al. (1990). Analytical errors are equal or smaller than the size of the symbols.

of the carbonates are reported relative to the Vienna Pedee Belemnite Standard (VPDB). XRD, TIC, C and O isotope data are compiled together with data from previous studies (Thornburg and Suess, 1992; Meister et al., 2007, 2008, 2011) in ESM Table S1.

3.2. Stable Mg-isotope analysis

Eight lithified carbonate samples and five unlithified bulk sediment samples were air-dried and finely ground using an agate mortar and pestle for the unlithified sediments or a disk mill for the lithified carbonates. Traces of biogenic calcite were removed after sample reaction with 0.1 M ethylenediaminetetraacetic acid (EDTA) solution (pH 6.3) (Meister et al., 2007). The Mg isotopic compositions of the ground carbonate samples were measured using the digestion procedure described by Pokrovsky et al. (2011). About 20 mg of powdered bulk sediment was digested in a 10 M nitric acid solution at 90 °C in sealed teflon vessels for 48 hours. Samples were then evaporated to dryness and re-dissolved in 1 M nitric acid prior to Mg isotope chromatographic separation by ion exchange. Similarly, the collected pore fluids were evaporated to dryness, re-dissolved in 0.25 mL 10 M HNO_3, again evaporated to dryness and dissolved again in 1 M HNO_3 prior to chromatographic separation.

About 20 μg of Mg from the solid and pore fluid samples was processed to separate Mg from the matrix elements. Samples were loaded into Bio-Rad poly-prep 10 mL columns containing 1 mL AG50W-X12 resin and eluted using 1 M HNO_3 (Mavromatis et al., 2013). More than 99% of the initial Mg was recovered by this process. The cation/Mg mass ratio of the samples prior to the isotopic analyses was <0.002 as determined by ICP-MS analysis. Magnesium isotopes were measured with a Thermo-Finnigan 'Neptune' MC-ICP-MS at GET (Géosciences Environement Toulouse, France). Mass fractionation effects of the instrument were corrected via sample-standard bracketing using the DSM3 standard, and all data are presented as δ^xMg values with respect to the DSM3 reference material [$\delta^x Mg = (({}^xMg / {}^{24}Mg)_{sample} / ({}^xMg / {}^{24}Mg)_{DSM3} - 1) \times 1000$] where x refers to the Mg mass of interest. The reproducibility of the DSM3 standard was typically better than 0.08‰ and was confirmed by replicate analyses of three Mg reference standards (DSM3, CAM-1 and OUMg) as shown in Table 2, resulting in values similar to those reported earlier (e.g. CAM-1: $\delta^{25}Mg = -1.343 \pm 0.048$‰, $\delta^{26}Mg = -2.592 \pm 0.087$‰ Tipper et al., 2008; OUMg $\delta^{25}Mg = -1.45 \pm 0.05$‰, $\delta^{26}Mg = -2.80 \pm 0.08$‰ Pearce et al., 2012). The validity of the method was assessed by passing monoelemental CAM-1 standard through column chemistry. In addition, the JDo-1 international standard material, processed together with the samples of this work, resulted in isotopic composition similar to that previously reported in the literature ($\delta^{25}Mg = -1.22 \pm 0.06$‰, $\delta^{26}Mg = -2.33 \pm 0.09$‰; Wombacher et al., 2009; Pearce et al., 2012; Mavromatis et al., 2013; Beinlich et al., 2014).

4. Results

The results of XRD analyses are presented in Table ESM-1. The results show that the lithified samples consist of dolomite with minor amounts of quartz, feldspar, and clay minerals, whereas the unlithified sediments consist of quartz, feldspar, and clay minerals. No calcite was

detected in either the dolomites or the unlithified sediment samples. Total inorganic carbon (TIC) in the unlithified sediments is less than 0.2 wt.% (Table ESM-1). Type I dolomites have a $\delta^{13}C$ around −30‰ and type II dolomites have a $\delta^{13}C$ around +10‰. Furthermore, Type I dolomites exhibit $\delta^{18}O$ values of about 4.5‰, whereas type II dolomite samples are characteristically enriched in ^{18}O with $\delta^{18}O$ values averaging ~6.5‰ (see Table ESM-1).

Representative scanning electron microphotographs of type I and type II dolomite are shown in Fig. 3. Type I dolomite exhibits a euhedral rhombic texture, whereas type II dolomite exhibits polygonal grain boundaries, suggesting that the crystals grew within cavities during fracturing.

Results of Mg isotope analyses of pore fluids, carbonates, and sediments from site 1230 are shown in Fig. 4 and listed in Tables 1 and 2. The $\delta^{26}Mg$ values of pore fluids increase with depth from −0.85‰ (DSM3) at the seafloor to about 1.0‰ at 140 mbsf. The pore fluid $\delta^{26}Mg$ remains essentially constant, with an average $\delta^{26}Mg$ of 0.78 ± 0.19‰ below 140 mbsf until the base of the sedimentary sequence at 250 mbsf. The $\delta^{26}Mg$ of dolomite samples ranged from −2.5‰ to −3.5‰ (see Table 1). These values are substantially depleted in ^{26}Mg compared to their adjacent pore fluids. The type I dolomite collected at 6.5 mbsf is the most depleted in ^{26}Mg with a $\delta^{26}Mg$ of −3.5‰ which is 0.5–1.0‰ lighter than the type II dolomites collected from ~230 mbsf with a $\delta^{26}Mg$ ranging between −2.5 and −3.0‰. A dolomite sample recovered from ~460 mbsf at Site 685 exhibits a $\delta^{26}Mg$ of −2.7‰, which falls within the range of type II dolomites. The $\delta^{26}Mg$ values of unlithified sediment containing only traces of carbonate recovered from various depths from Sites 1230 and 685 range between −0.3‰ and 0.1‰.

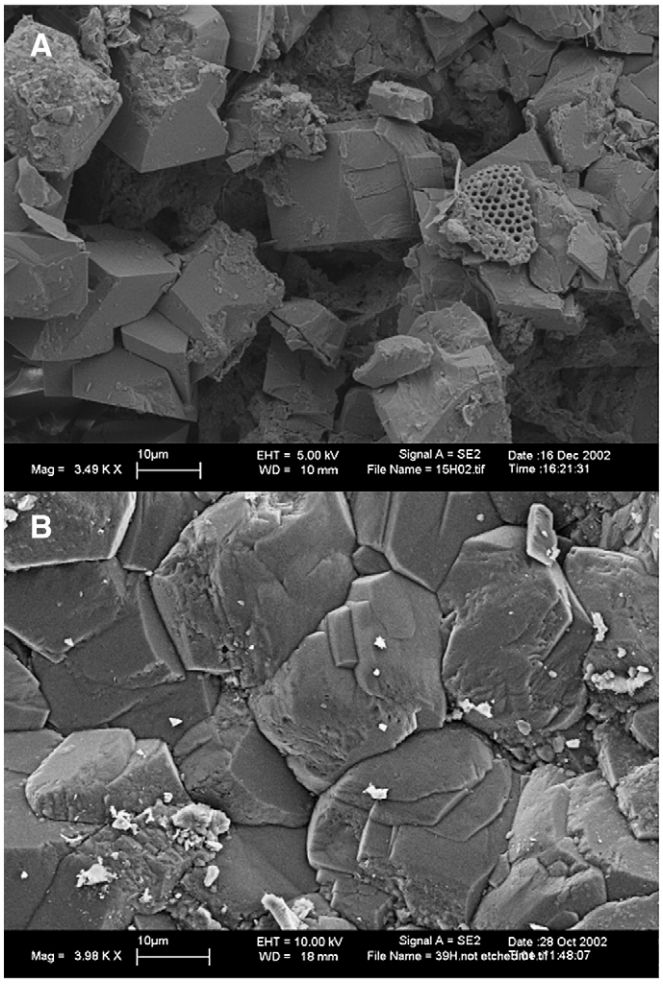

Fig. 3. Characteristic scanning electron microphotographs of diagenetic dolomite recovered from A) ~6 mbsf Peru shelf (type I) and B) ~230 mbsf Site 1230 (type II).

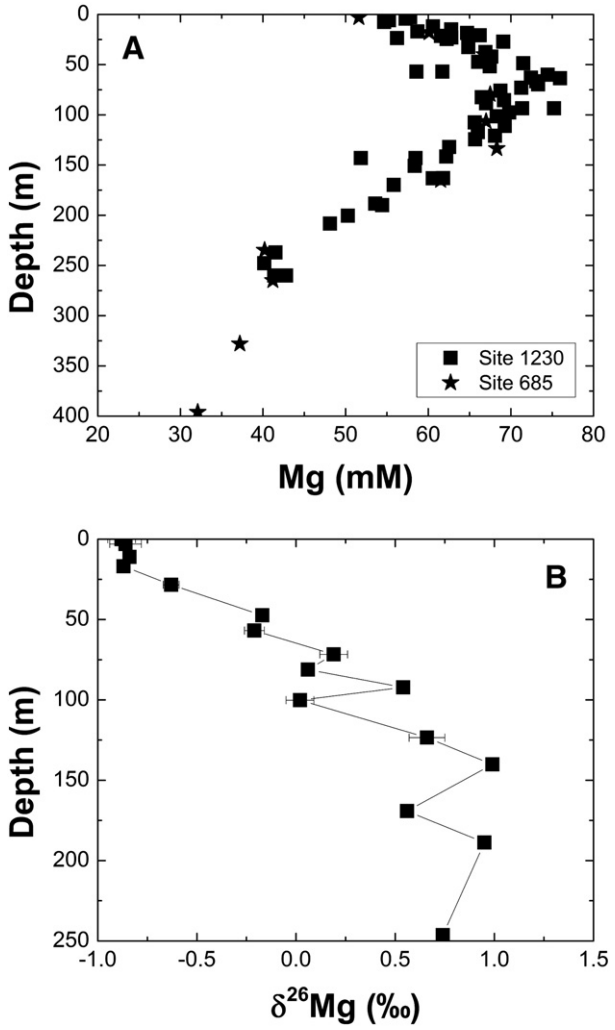

Fig. 4. Measured Mg concentration (A) and Mg stable isotope composition (B) of pore fluids in ODP Site 1230 and Site 685. Analytical errors during isotopic analyses (2σ) are included in the sings of the plot. If not shown, analytical errors are equal or smaller than the size of the symbols.

5. Discussion

5.1. Interaction of sediments with pore fluids

The Mg-isotope composition of the pore fluids provides insight into the diagenetic processes occurring in this system. The $\delta^{26}Mg$ values of the pore fluid within the top ~17 mbsf average −0.86‰ and are similar to that of seawater (i.e. −0.83‰; Foster et al., 2010). This observation suggests that the pore-water composition is strongly influenced by the downward migration of seawater. Below this depth, $\delta^{26}Mg$ values (Fig. 4) increase. Von Breymann et al. (1990) argued that the increase of pore fluid Mg concentration with depth at Site 1230 stems from Mg exchange from clay mineral surfaces with the NH_4 produced by organic matter degradation. Alternatively, Wallmann et al. (2008) suggested that silicate mineral dissolution contributes Mg to the pore fluid. It is generally accepted that terrigenous silicates are enriched in ^{26}Mg compared to seawater (Young and Galy, 2004; Tipper et al., 2006; Teng et al., 2007; Pogge von Strandmann et al., 2008; Teng et al., 2010). Furthermore, it has recently been shown that ^{26}Mg preferentially adsorbs on

Table 1
Mg isotope composition of analyzed unlithified sediments and carbonates recovered from Sites 685 and 1230, relative to DSM3. Uncertainties are reported as twice the standard deviation (2SD) of "n" replicates.

Core-section, Interval (cm)	Depth (mbsf)	Description	Mineralogy		δ^{25}Mg (‰)	2σ	δ^{26}Mg (‰)	2σ	n	Comments
			Main components	Traces						
Unlithified sediment										
685A-44X-1, 142-146	394.0	Unlith. sediment			0.03	0.07	0.08	0.09	3	
685A-50X-CC, 30-32	450.9	Semi-lith. mud			−0.01	0.01	−0.03	0.07	3	
1230A-4H-5WR, 70-75	30.6	Unlith. sediment			−0.17	0.04	−0.32	0.04	3	
1230A-22H-3WR, 70-75	172.0	Unlith. sediment			−0.16	0.02	−0.30	0.02	3	
1230A-37X-1, 65-70	258.3	Unlith. sediment			−0.03	0.02	−0.03	0.03	3	
Carbonates										
685A-2H-2, 45-60	6.5	Nodule	Dolomite, Quartz	Plagioclase	−1.82	0.06	−3.46	0.06	3	Type I
685A-51X-CC, 1-3	459.1	Nodule	Dolomite	Quartz	−1.48	0.04	−2.7	0.01	3	Type II
1230A-33X-1, 46-49	234.9	Nodule	Dolomite	Quartz, calcite	−1.49	0.01	−2.86	0.03	3	Type II
1230A-33X-1, 46-49	234.9				−1.58	0.04	−3.03	0.08	3	Type II, Leached
1230A-30X-1, 0-5	226.3	Nodule	Dolomite	Quartz	−1.4	0.03	−2.67	0.09	3	Type II, Leached
1230A-30X-CC, 22-25	228.0	Nodule	Dolomite	Quartz	−1.32	0.02	−2.54	0.01	3	Type II, Leached
1230A-31X-1, 0-19	229.6	Dolomite layer, top	Dolomite	Quartz	−1.35	0.02	−2.62	0.02	3	Type II
	229.6	Dolomite layer, bottom	Dolomite	Quartz	−1.36	0.03	−2.61	0.03	3	Type II, Leached

the surfaces of kaolinite type minerals (Huang et al., 2012; Opfergelt et al., 2014). Thus, both dissolution and desorption of exchangeable Mg from clay minerals could lead to the observed pore fluid δ^{26}Mg increase with depth.

To estimate the contribution of Mg from silicates to the Mg-isotope composition of the pore fluid, the Mg isotope compositions of five unlithified sediment samples collected from different depths were determined. The Mg isotope composition of these sediments (Fig. 3 and Table 1) falls within the range of −0.3 to 0.1‰ (DSM3). These values are consistent with the Mg isotope composition of silicate and clay minerals reported in previous studies (e.g. 0.0 to −0.3‰; Young and Galy, 2004; Tipper et al., 2006; Teng et al., 2007; Pogge von Strandmann et al., 2008; Teng et al., 2010) and they are more positive than in seawater. Note that our samples contain less than 0.2 wt.% total inorganic carbon, probably of marine origin (calcite) but its presence is unlikely to have influenced the measured Mg isotope compositions. These observations indicate that the conservative dissolution of clay minerals cannot alone explain the ^{26}Mg of up to 0.8‰ as observed below ~100 mbsf.

Desorption of ^{26}Mg due to ion exchange with NH_4^+ on clay mineral surfaces is another possible mechanism leading to enrichment of pore fluids with ^{26}Mg. Indeed, previous studies (Huang et al., 2012; Opfergelt et al., 2014) have recorded δ^{26}Mg values in clay-adsorbed Mg of up to 1‰. If indeed, as suggested by Von Breymann et al. (1990), Mg-release is due to cation exchange, a different Mg pool than the isotopic light pool from leachates could have affected the pore fluid. Note here that, if it is assumed that the pore fluid Mg-isotope composition represents only a mixture of seawater-derived Mg and Mg desorbed from clay minerals, mass balance calculations using the fluid concentration at ~150 mbsf (e.g. 70 mM) and its average Mg isotope composition would require a δ^{26}Mg value for adsorbed Mg of 6.6‰, which is dramatically higher than that of the bulk sediment. It therefore seems unlikely that ion exchange alone leads to the observed ^{26}Mg enrichment in the pore fluids within the top 200 mbsf. This conclusion is consistent with the plot of Mg concentrations versus δ^{26}Mg values of pore fluids (Fig. 5) which does not show a linear relationship, but rather indicates the presence of at least one additional Mg isotope fractionating process in the system.

Table 2
Sample depth, total Mg concentration and Mg isotope composition of pore fluids and reference material used during this study, relative to DSM3. Uncertainties are reported as twice the standard deviation (2SD) of "n" replicates.

Core-section, Interval (cm)	Depth (mbsf)	Mg (mM)	δ^{25}Mg (‰)	2σ	δ^{26}Mg (‰)	2σ	n
1230B-1-1, 0-15	0.0	55	−0.46	0.09	−0.88	0.07	3
1230B-2-1, 0-5	3.0	55	−0.45	0.08	−0.86	0.08	3
1230B-2-6, 60-75	11.1	59	−0.42	0.04	−0.84	0.02	3
1230B-3-3, 135-150	16.9	59	−0.48	0.01	−0.87	0.02	3
1230B-5-3, 135-150	28.4	62	−0.37	0.03	−0.63	0.04	3
1230D-7-3, 135-150	47.4	66	−0.11	0.03	−0.17	0.03	3
1230B-8-3, 135-150	56.9	62	−0.16	0.03	−0.21	0.05	3
1230A-10-1, 135-150	71.7	71	0.06	0.01	0.19	0.07	3
1230A-11-3, 135-150	81.2	66	−0.03	0.03	0.06	0.03	3
1230A-12-2, 135-150	92.2	72	0.25	0.04	0.54	0.03	3
1230A-13-1, 135-150	100.2	68	0.01	0.03	0.02	0.07	3
1230A-15-5, 90-100	123.5	65	0.36	0.05	0.66	0.09	3
1230A-18-1, 135-150	140.2	62	0.45	0.01	0.99	0.02	3
1230A-22-1, 85-90	169.2	55	0.27	0.01	0.56	0.01	3
1230A-24-2, no interval	188.8	53	0.47	0.02	0.95	0.02	3
1230A-35-1, 135-150	246.4	40	0.36	0.03	0.74	0.03	3
DSM3			0.01	0.03	0.02	0.05	54
CAM-1			−1.32	0.07	−2.61	0.08	12
CAM-1[a]			−1.35	0.06	−2.63	0.05	3
OUMg			−1.42	0.05	−2.84	0.08	12
JDo-1			−1.25	0.06	−2.36	0.06	6

[a] Sample passed through column separation.

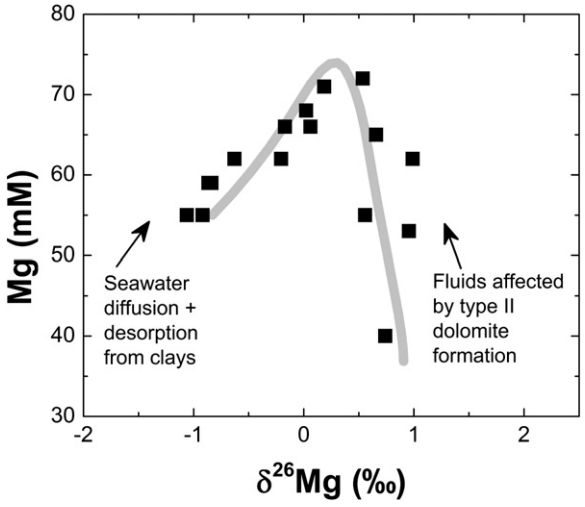

Fig. 5. Plot of δ^{26}Mg vs. Mg concentration of pore fluids. The arrows indicate the processes affecting Mg chemical and isotopic composition in the pore fluids. Analytical errors are equal or smaller than the size of the symbols.

Below ~230 mbsf and below the zone of intense methanogenesis, pore fluid Mg concentration decreases steadily toward 28 mM at 450 mbsf (see Fig. 2) while the Ca concentration increases with depth. High Ca/low Mg content is not consistent with modern seawater but rather indicates the influence of an altered fluid at depth. This is also suggested by increasingly radiogenic Sr isotope values in the pore fluid toward the base of the sequence (Kastner et al., 1990). Furthermore, deep fluids advecting laterally along a décollement (Matmon and Bekins, 2006) may have been present at some time in the past, although Cl^- profiles do not suggest this at present.

At ~230 mbsf however, the change of the slope of pore fluid Mg and Ca indicates a sink of these two ions from the solution. This observation is consistent with the precipitation of a 20 cm thick dolomite layer as previously described at this depth (Meister et al., 2011). Based on its location at the décollement, its synkinematic fabrics, and radiogenic Sr isotope composition, it has been concluded that this dolomite precipitation was induced by upward advection of deeply sourced fluids along the décollement (Kastner et al., 1990; Meister et al., 2011). Note here that dolomite formation has earlier been shown to enrich the porefluids in ^{26}Mg, due to preferential uptake of ^{24}Mg during carbonate mineral forming (Higgins and Schrag, 2010; Beinlich et al., 2014). Hence the pore fluid enrichment in ^{26}Mg is related to dolomite-fluid Mg isotope fractionation and the extent of Mg removal from pore fluid.

Note that the enrichment in ^{26}Mg in pore fluids at ~230 mbsf is unlikely to occur due to the influence of deep-sourced fluids. At the depths where the deep-sourced fluid originated, clay mineral transformation leads to the enrichment of pore fluids in Ca and depletion in Mg; clay mineral formation has earlier been shown to deplete Mg in pore fluids and decrease significantly its δ^{26}Mg composition (Higgins and Schrag, 2010).

5.2. Magnesium isotope fractionation during dolomite formation

All dolomite samples analyzed in this study are depleted in ^{26}Mg compared to their adjacent pore fluids. This behaviour is in agreement with previous observations indicating the preferential incorporation of light Mg in Mg-bearing carbonates (Galy et al., 2002; Buhl et al., 2007; Hippler et al., 2009; Immenhauser et al., 2010; Wombacher et al., 2011; Pearce et al., 2012; Mavromatis et al., 2012a, 2013; Shirokova et al., 2013; Beinlich et al., 2014).

Authigenic dolomite formation at Site 1230 occurs at ~6.5 mbsf and at ~230 mbsf. The shallow, type I dolomite formation has been attributed to AOM at the modern sulfate–methane transition (SMT) zone (Meister et al., 2011). This shallow SMT forms as a result of high organic carbon turnover rates and a large methane flux from below (cf. Meister et al., 2013). Based on the steep sulfate and methane gradients, turnover rates are enhanced in this zone, resulting in the rapid alkalinity production that promotes early diagenetic dolomite precipitation. The dolomite forming at 6.5 mbsf has a δ^{26}Mg of −3.5‰ (DSM3), which is ~2.5‰ lower than that of its co-existing pore fluids. Based on the pore fluid δ^{26}Mg (Fig. 2) and the fact that dolomite precipitation at the SMT is also Ca-limited (cf. Baker and Burns, 1985; Compton, 1988) it seems likely that the pore fluids are influenced by a downward diffusion of seawater. The apparent dolomite–pore fluid fractionation factor ($\Delta^{26}Mg_{Dol\text{-}fluid} = \delta^{26}Mg_{Dol} - \delta^{26}Mg_{fluid}$) in this system is −2.6‰, which is within the range of fractionation factors proposed by Higgins and Schrag (2010), but about 1‰ smaller than that generated from the ab-initio calculations of Schauble (2011) for 2 °C (i.e. −3.6‰), the ambient temperature of the sediment–water interface. This discrepancy between our observations and the ab-initio calculations might imply that the measured apparent fractionation factor may be affected by kinetic effects (Immenhauser et al., 2010; Mavromatis et al., 2013) or reflect uncertainties in the ab-initio calculations.

Type I dolomite commonly occurs in organic carbon-rich hemipelagic sediments (cf. Thornburg and Suess, 1992; Moore et al., 2004; Meister et al., 2006, 2007, 2008; Ussler and Paull, 2008). No type I dolomites, however, are observed deeper at Site 1230. It seems likely that if dolomite was ever present deeper, it dissolved upon burial into the methanogenic zone due to acidification by CO_2. Mg released from dissolving dolomite would have contributed isotopically light Mg to the pore fluid, but the absence of isotopically light Mg measured in the sampled pore fluids rather suggests that this is not a dominant process.

The type II dolomites occurring at ~230 mbsf have δ^{26}Mg values that range between −2.5 and −3.0‰, and are more than 3.3‰ lower than the adjacent pore fluids. As it is discussed above (see Section 5.1), it is expected that the δ^{26}Mg composition of deeply sourced fluids was lower than that currently sampled at this depth. Taking this possibility into account, it is possible that the Mg isotope composition of the sample pore fluid and associated type II dolomites might have been influenced by carbonate mineral formation in a semi-closed pore fluid system (e.g. Rayleigh-type fractionation), where Ca and alkalinity were supplied episodically along the décollement and induced dolomite precipitation. The absence of further measurements, however, does not allow at the moment an estimation of the Mg isotope fractionation factor between type II dolomite and pore fluid. Note here that a number of additional processes could have influenced the Mg isotope composition of type II dolomites. These include i) fast precipitation reactions, which have been shown to influence significantly the isotopic composition of precipitating carbonates (Mavromatis et al., 2013) and are in agreement with the xenotopic crystal structures (Fig. 2B) exhibited by these dolomites, ii) variations in Mg fractionation factors in response to changing fluid concentrations including the presence of organic substances (cf. Mavromatis et al., 2011) and are in agreement with the enriched in DOC pore fluid with contents up to 20 mM (Smith, 2005) at this depth. An additional possibility is that the current porefluid differs in its Mg isotopic composition from that occurred during dolomite precipitation, as suggested by its chloride concentration (see above).

5.3. Implications for the geological record

The observed difference in the δ^{26}Mg composition between shallow (type I) and deeply forming (type II) dolomite is between 0.5 and 1‰. Although small, this difference in isotope composition between the two dolomite types helps to better constrain the Mg isotope fractionation behavior during early diagenetic dolomite formation. δ^{26}Mg values similar to that of the type II dolomites at Site 1230 have been observed in the dolomites at ODP Sites 1012 (California Margin), and even less negative values have been observed for dolomites at Site 1082 (Benguela Current; Higgins and Schrag, 2010). At these sites,

dolomite formation was considered responsible for ^{26}Mg enrichment in the pore fluid due to a Rayleigh fractionation effect in a semi-closed system. The discussion above, however, suggests that there are several additional processes that could have led to these observed Mg isotopic compositions. In contrast, the type I dolomite forming within the near subsurface sediments at Site 1230 has probably been formed directly from seawater.

Although additional Mg isotope measurements of type I dolomites would further illuminate the fractionation process, the difference in the isotopic composition between shallow open-system dolomites and deeply forming diagenetic dolomites may provide a new tool to discriminate dolomite formation conditions. Despite their similar apparent Mg isotope fractionation factor, the observed variations in $\delta^{26}Mg$ composition of the two types of dolomite, together with their distinctive $\delta^{13}C$ composition, can be used to diversify dolomite formation environments in geological archives. Type II dolomite formation is characterized by $\delta^{26}Mg > -3.0‰$ and $4‰ < \delta^{13}C < 13‰$. (Meister et al., 2011; Higgins and Schrag, 2010; this study). In contrast type I dolomites are enriched in ^{24}Mg ($\delta^{26}Mg < -3.0‰$) and exhibit $\delta^{13}C < -30‰$, which is typical for carbonates formed due to dissimilatory organic matter degradation probably in relation to AOM. The combination of these two isotopic systems may provide a new tool to distinguish dolomites formed during AOM (type I) from those associated with altered fluids and greater depth and within the zone of methanogenesis (type II).

6. Conclusions

The dolomites occurring at Site 1230, Peru margin, can be divided into two types based on their texture, isotope content, and diagenetic process leading to their formation. Type I dolomite forms due to anaerobic methane oxidation in the shallow subsurface near the sulfate–methane transition zone, whereas type II dolomite forms deep within the methanogenic zones due to the upward migration of Ca-rich fluids along the décollement. Type I dolomite exhibits $\delta^{26}Mg$ of $-3.5‰$ and is characterized by an apparent Mg isotope fractionation factor of $-2.6‰$. Type II dolomites have $\delta^{26}Mg$ values $> -3.0‰$ and are significantly lighter than the modern pore fluid Mg isotope composition. The observed enrichment of pore fluid below ~200 mbsf in ^{26}Mg could stem from a number of processes including i) the influence of dolomite formation in a semi-closed system, ii) a change in fluid composition following its deposition and iii) kinetic isotope effects. Other processes, such as clay mineral alteration and/or inflow of ^{26}Mg-enriched deeply sourced fluids, also play a role in the Mg isotope composition of the pore fluids within the methanogenic zone. As Mg isotope signatures appear to allow the distinction between shallow (type I) versus deeper (type II) dolomites they may provide a useful palaeo-diagenetic proxy.

Acknowledgments

For his support with Mg isotope analyses we thank Jerome Chmeleff. We thank Monika Segl and Gaute Lavik for providing additional $\delta^{13}C$ data from dolomites and Andrea Schipper for TIC/TOC measurements. This research used samples and data provided by the Integrated Ocean Drilling Program (IODP). This study was funded through EU Collaborative project CarbFix (FP7-ENERGY-2011-1-283148), the Marie Curie Research and Training Network Greenhouse-Gas Removal Apprenticeship and Student Program (GRASP; project MRTN-CT-2006-035868), and the Swiss National Science Foundation (SNF, project PA00P2-126221). The editor M. Böttcher and the reviewers E. Tipper and F. Wombacher are thankfully acknowledged for their constructive comments.

Appendix A. Supplementary data

Supplementary data to this article can be found online at http://dx.doi.org/10.1016/j.chemgeo.2014.07.019.

References

Azmy, K., Lavoie, D., Wang, Z., Brand, U., Al-Aasm, I., Jackson, S., Girard, I., 2013. Magnesium-isotope and REE compositions of Lower Ordovician carbonates from eastern Laurentia: implications for the origin of dolomites and limestones. Chem. Geol. 356, 64–75.

Baker, P.A., Burns, S.J., 1985. Occurrence and formation of dolomite in organic-rich continental margin sediments. AAPG Bull. 69, 1917–1930.

Beinlich, A., Mavromatis, V., Austrheim, H., Oelkers, E.H., 2014. Inter-mineral Mg isotope fractionation during hydrothermal ultramafic rock alteration—implications for the global Mg-cycle. Earth Planet. Sci. Lett. 392, 166–176.

Buhl, D., Immenhauser, A., Smeulders, G., Kabiri, L., Richter, D.K., 2007. Time series $\delta^{26}Mg$ analysis in speleothem calcite: Kinetic versus equilibrium fractionation, comparison with other proxies and implications for palaeoclimate research. Chem. Geol. 244, 715–729.

Compton, J.S., 1988. Degree of supersaturation and precipitation of organogenic dolomite. Geology 16, 318–321.

D'Hondt, S., Jørgensen, B.B., Miller, J., ODP Leg 201 Shipboard Scientific Party, 2003. Controls on microbial communities in deeply buried sediments, Eastern Equatorial Pacific and Peru Margin, Sites 1225–1231. Proc. ODP, Init. Repts., v. 201. College Station, TX.

Donohue, C.M., Snyder, G.T., Dickens, G.R., 2006. Data report: major cation concentrations of interstitial waters collected from deep sediments of Eastern Equatorial Pacific and Peru Margin (ODP Leg 201). Proc. ODP, Sci. Results., v. 201. Ocean Drilling Program, College Station, TX.

Foster, G.L., von Strandmann, P., Rae, J.W.B., 2010. Boron and magnesium isotopic composition of seawater. Geochem. Geophys. Geosyst. 11, 10.

Galy, A., Bar-Matthews, M., Halicz, L., O'Nions, R.K., 2002. Mg isotopic composition of carbonate: insight from speleothem formation. Earth Planet. Sci. Lett. 201, 105–115.

Hensen, C., Wallmann, K., Schmidt, M., Ranero, C.R., Suess, E., 2004. Fluid expulsion related to mud extrusion off Costa Rica—a window to the subducting slab. Geology 32, 201–204.

Higgins, J.A., Schrag, D.P., 2010. Constraining magnesium cycling in marine sediments using magnesium isotopes. Geochim. Cosmochim. Acta 74, 5039–5053.

Hippler, D., Buhl, D., Witbaard, R., Richter, D.K., Immenhauser, A., 2009. Towards a better understanding of magnesium-isotope ratios from marine skeletal carbonates. Geochim. Cosmochim. Acta 73, 6134–6146.

Huang, K.J., Teng, F.Z., Wei, G.J., Ma, J.L., Bao, Z.Y., 2012. Adsorption- and desorption-controlled magnesium isotope fractionation during extreme weathering of basalt in Hainan Island, China. Earth Planet. Sci. Lett. 359, 73–83.

Immenhauser, A., Buhl, D., Richter, D., Niedermayr, A., Riechelmann, D., Dietzel, M., Schulte, U., 2010. Magnesium-isotope fractionation during low-Mg calcite precipitation in a limestone cave—field study and experiments. Geochim. Cosmochim. Acta 74, 4346–4364.

Inagaki, F., Nunoura, T., Nakagawa, S., Teske, A., Lever, M., Lauer, A., Suzuki, M., Takai, K., Delwiche, M., Colwell, F.S., Nealson, K.H., Horikoshi, K., D'Hondt, S., Jørgensen, B.B., 2006. Biogeographical distribution and diversity of microbes in methane hydrate-bearing deep marine sediments on the Pacific Ocean Margin. Proc. Natl. Acad. Sci. 103, 2815–2820.

Kastner, M., Elderfield, H., Martin, J.B., Suess, E., Kvenvolden, K.A., Garrison, R.E., 1990. Diagenesis and interstitial-water chemistry at the Peruvian Continental Margin—major constituents and strontium isotopes. In: Suess, E., von Huene (Eds.), Proc ODP, Sci Results, v. 112. Ocean Drilling Program, College Station, TX, pp. 413–440.

Li, W., Chakraborty, S., Beard, B.L., Romanek, C.S., Johnson, C.M., 2012. Magnesium isotope fractionation during precipitation of inorganic calcite under laboratory conditions. Earth Planet. Sci. Lett. 333–334, 304–316.

Matmon, D., Bekins, B., 2006. Hydromechanics of a high taper angle, low-permeability prism: a case study from Peru. J. Geophys. Res. 111, B07101. http://dx.doi.org/10.1029/2005JB003697.

Mavromatis, V., Gautier, Q., Schott, J., Oelkers, E.H., 2011. Effect of aqueous organic ligands on Mg-isotope fractionation during magnesite precipitation. Goldschmidt 2011, Prague, Czech Republic. Mineral. Mag. 75, 1430.

Mavromatis, V., Pearce, C.R., Shirokova, L.S., Bundeleva, I.A., Pokrovsky, O.S., Benezeth, P., Oelkers, E.H., 2012a. Magnesium isotope fractionation during hydrous magnesium carbonate precipitation with and without cyanobacteria. Geochim. Cosmochim. Acta 76, 161–174.

Mavromatis, V., Botz, R., Schmidt, M., Liebetrau, V., Hensen, C., 2012b. Formation of carbonate concretions in surface sediments of two mud mounds, offshore Costa Rica—a stable isotope study. Int. J. Earth Sci. 1–14.

Mavromatis, V., Gautier, Q., Bosc, O., Schott, J., 2013. Kinetics of Mg partition and Mg stable isotope fractionation during its incorporation in calcite. Geochim. Cosmochim. Acta 114, 188–203.

Meister, P., McKenzie, J.A., Warthmann, R., Vasconcelos, C., 2006. Mineralogy and petrography of diagenetic dolomite from the ODP Leg 201 Peru Margin drill sites. Proc. ODP, Sci. Results, v. 201. Ocean Drilling Program, College Station, TX (online publ.: http://www-odp.tamu.edu/publications/201_SR/102/102.htm).

Meister, P., McKenzie, J.A., Vasconcelos, C., Bernasconi, S., Frank, M., Gutjahr, M., Schrag, D.P., 2007. Dolomite formation in the dynamic deep biosphere: results from the Peru Margin. Sedimentology 54, 1007–1031.

Meister, P., Bernasconi, S.M., Vasconcelos, C., McKenzie, J.A., 2008. Sealevel changes control diagenetic dolomite formation in hemipelagic sediments of the Peru Margin. Mar. Geol. 252, 166–173.

Meister, P., Gutjahr, M., Frank, M., Bernasconi, S.M., Vasconcelos, C., McKenzie, J.A., 2011. Dolomite formation within the methanogenic zone induced by tectonically driven fluids in the Peru accretionary prism. Geology 39, 563–566.

Meister, P., Liu, B., Ferdelman, T.G., Jorgensen, B.B., Khalili, A., 2013. Control of sulphate and methane distributions in marine sediments by organic matter reactivity. Geochim. Cosmochim. Acta 104, 183–193.
Moore, T.S., Murray, R.W., Kurtz, A.C., Schrag, D.P., 2004. Anaerobic methane oxidation and the formation of dolomite. Earth Planet. Sci. Lett. 229, 141–154.
Opfergelt, S., Burton, K.W., Georg, R.B., West, A.J., Guicharnaud, R.A., Sigfusson, B., Siebert, C., Gislason, S.R., Halliday, A.N., 2014. Magnesium retention on the soil exchange complex controlling Mg isotope variations in soils, soil solutions and vegetation in volcanic soils, Iceland. Geochim. Cosmochim. Acta 125, 110–130.
Pearce, C.R., Saldi, G.D., Schott, J., Oelkers, E.H., 2012. Isotopic fractionation during congruent dissolution, precipitation and at equilibrium: evidence from Mg isotopes. Geochim. Cosmochim. Acta 92, 170–183.
Pogge von Strandmann, P.A.E., Burton, K.W., James, R.H., van Calsteren, P., Gislason, S.R., Sigfusson, B., 2008. The influence of weathering processes on riverine magnesium isotopes in a basaltic terrain. Earth Planet. Sci. Lett. 276, 187–197.
Pokrovsky, B.G., Mavromatis, V., Pokrovsky, O.S., 2011. Co-variation of Mg and C isotopes in late Precambrian carbonates of the Siberian Platform: a new tool for tracing the change in weathering regime? Chem. Geol. 290, 67–74.
Riechelmann, S., Buhl, D., Schroder-Ritzrau, A., Spötl, C., Riechelmann, D.F.C., Richter, D.K., Kluge, T., Marx, T., Immenhauser, A., 2012. Hydrogeochemistry and fractionation pathways of Mg isotopes in a continental weathering system: lessons from field experiments. Chem. Geol. 300, 109–122.
Schauble, E.A., 2011. First-principles estimates of equilibrium magnesium isotope fractionation in silicate, oxide, carbonate and hexaaquamagnesium(2+) crystals. Geochim. Cosmochim. Acta 75, 844–869.
Shirokova, L.S., Mavromatis, V., Bundeleva, I.A., Pokrovsky, O.S., Benezeth, P., Gerard, E., Pearce, C.R., Oelkers, E.H., 2013. Using Mg isotopes to trace cyanobacterially mediated magnesium carbonate precipitation in alkaline lakes. Aquat. Geochem. 19, 1–24.
Smith, D.C., 2005. Data report: dissolved organic carbon in interstitial waters, equatorial Pacific and Peru margin, ODP Leg 201. In: Jørgensen, B.B., D'Hondt, S.L., Miller, D.J. (Eds.), Proc. ODP, Sci. Results, 201, pp. 1–10.
Spivack, A.J., McNeil, C., Holm, N.G., Hinrichs, K.-U., 2006. Determination of in situ methane based on analysis of void gas. In: Jørgensen, B.B., D'Hondt, S.L., Miller, D.J. (Eds.), Proc. ODP, Sci. Results, 201, pp. 1–11 ((online). Available from http://www-odp.tamu.edu/publications/201_SR/VOLUME/CHAPTERS/119.PDF).
Suess, E., von Huene, R., ODP Leg 112 Shipboard Scientific Party, 1990. Peru continental margin. Proc. ODP, Init. Repts., 112. Ocean Drilling Program, College Station, TX.
Teng, F.Z., Wadhwa, M., Helz, R.T., 2007. Investigation of magnesium isotope fractionation during basalt differentiation: implications for a chondritic composition of the terrestrial mantle. Earth Planet. Sci. Lett. 261, 84–92.
Teng, F.Z., Li, W.Y., Rudnick, R.L., Gardner, L.R., 2010. Contrasting lithium and magnesium isotope fractionation during continental weathering. Earth Planet. Sci. Lett. 300, 63–71.
Thornburg, T.M., Suess, E., 1992. Carbonate cementation of granular and fracture porosity: implications for the Cenozoic hydrologic development of the Peru Continental Margin. In: Suess, M. (Ed.), Proceedings of the Ocean Drilling Program, Scientific results, v. 112, pp. 95–109.
Tipper, E.T., Galy, A., Bickle, M.J., 2006. Riverine evidence for a fractionated reservoir of Ca and Mg on the continents: implications for the oceanic Ca cycle. Earth Planet. Sci. Lett. 247, 267–279.
Tipper, E.T., Louvat, P., Capmas, F., Galy, A., Gaillardet, J., 2008. Accuracy of stable Mg and Ca isotope data obtained by MC-ICP-MS using the standard addition method. Chem. Geol. 257, 65–75.
Ussler III, W., Paull, C.K., 2008. Rates of anaerobic oxidation of methane and authigenic carbonate mineralization in methane-rich deep-sea sediments inferred from models and geochemical profiles. Earth Planet. Sci. Lett. 266, 271–287.
Von Breymann, M.T., Collier, R., Suess, E., 1990. Magnesium adsorption and ion exchange in marine sediments: a multi-component model. Geochim. Cosmochim. Acta 54, 3295–3313.
Von Huene, R., Pecher, I.A., Gutscher, M.-A., 1996. Development of the accretionary prism along Peru and material flux after subduction of Nazca Ridge. Tectonics 15, 19–33.
Wallmann, K., Aloisi, G., Haeckel, M., Tishchenko, P., Pavlova, G., Greinert, J., Kutterolf, S., Eisenhauer, A., 2008. Silicate weathering in anoxic marine sediments. Geochim. Cosmochim. Acta 72, 3067–3090.
Wombacher, F., Eisenhauer, A., Heuser, A., Weyer, S., 2009. Separation of Mg, Ca and Fe from geological reference materials for stable isotope ratio analyses by MC-ICP-MS and double-spike TIMS. J. Anal. At. Spectrom. 24, 627–636.
Wombacher, F., Eisenhauer, A., Böhm, F., Gussone, N., Regenberg, M., Dullo, W.C., Rüggeberg, A., 2011. Magnesium stable isotope fractionation in marine biogenic calcite and aragonite. Geochim. Cosmochim. Acta 75, 5797–5818.
Yoshimura, T., Tanimizu, M., Inoue, M., Suzuki, A., Iwasaki, N., Kawahata, H., 2011. Mg isotope fractionation in biogenic carbonates of deep-sea coral, benthic foraminifera, and hermatypic coral. Anal. Bioanal. Chem. 401, 2755–2769.
Young, E.D., Galy, A., 2004. The isotope geochemistry and cosmochemistry of magnesium. In: Johnson, C.M., Beard, B.L., Albarede, F. (Eds.), Reviews in Mineralogy and Geochemistry. Mineralogical Soc America, pp. 197–230.